

Figure S6: Post entrapment crystallization corrections of olivine-hosted melt inclusions

The compositions of melt inclusions (MIs) in olivines were corrected in three distinct steps for post-entrapment crystallization (PEC) and for Fe-loss by using Petrolog 3 program [1]. First, at **Step 1**, oxide results from EMPA on MIs are inserted as input data in Petrolog 3 by using a targeted FeO^* value that approximate the FeOT/MgO tendency of magma composition and $\text{Fe}^{3+}/\Sigma\text{Fe}$ ratio of corresponding bulk rock composition determined by ICP-OES/MS. The data are plotted in a FeOT vs. MgO diagram, then at **Step 2**, after PEC correction is applied, the new Petrolog 3 output data are compared with bulk rock and matrix glass ratio FeOT/MgO . Finally, at **Step 3**, the FeOT data are adjusted for the KD of olivine-melt after PEC correction, therefore Mg\# from inclusion follow in equilibrium Fo\% from olivines. The major element concentrations after PEC correction were then recalculated on a 100% volatile free basis. The three steps are detailed as follows:

Step 1: Independently of the $\text{Fe}^{3+}/\Sigma\text{Fe}$ ratio, the targeted total iron species FeO^* value input in Petrolog 3 is adjusted with our ΣFe , which we consider equivalent to the EMPA results at each inclusion before PEC. The major element concentrations FeO (Fe^{2+}) and Fe_2O_3 (Fe^{3+}) were first estimated considering the $\text{Fe}^{3+}/\Sigma\text{Fe}$ ratio of the corresponding bulk rock sample composition. Total iron is reported by ICP-MS, while the ferrous iron is reported by fluorine (titration) (method of Saikkonen and I.A. Rautiainen (1993) [2]), as reported in Table S2.

The targeted melt $\text{Fe}^{3+}/\Sigma\text{Fe}$ ratio was fixed at the Ni–NiO buffer (NNO) in Petrolog 3 by following the model of Kress and Carmichael (1988) [3]. The NNO condition was preferred, since it represents various magmatic systems in arc magmas (e.g., [4]).

Step 2: The $\text{Fe}^{3+}/\Sigma\text{Fe}$ ratio from major oxides as Petrolog 3 output is susceptible to show data outside the KD error of olivine-melt as inconsistencies in FeO versus MgO tendency. For this reason, the general tendency of FeOT/MgO is verified between original and corrected PEC values to indicate the presence of co-genetic crystallizing behavior between MIs, bulk rock and groundmass [1, 5,6].

The melt oxidation state model of Kress and Carmichael (1988) [3] are expected to fit the error of original non-corrected PEC MIs. Error bars represent pure minimum Fe^{2+} content according to the $\text{Fe}^{3+}/\Sigma\text{Fe}$ ratio of the corresponding bulk rock sample. Each inclusion could represent a modelled ΣFe susceptible to follow variations in both Fe^{2+} and Fe^{3+} (figure 1a).

Step 3: An equilibrium Fe-Mg distribution coefficient KD was used between olivine and liquid (KD of $\text{Fe-Mg}_{\text{ol-liq}}$ of 0.30 [7], incrementally adding the olivine composition to the MI until the equilibrium KD value (0.30) with the host olivine was reached (figure 1b). To better compare the data set before and after PEC corrections, lines representing different KD of $\text{Fe-Mg}_{\text{ol-liq}}$ (0.27 and 0.33) were also calculated. The FeOT data is adjusted for the KD of olivine-melt, therefore Mg\# from inclusion follow a proportional relationship with Fo\% from olivine. The major element concentrations after PEC were then recalculated on a 100% volatile free basis. It is assumed that olivine contains negligible Fe^{3+} in comparison to ΣFe , which implies that Fe^{3+} representing the liquid melt is expected to be low [8]. In relatively reduced systems, KD that consider Fe^{2+} can be used with confidence, assuming that $\text{Fe}^{2+} = \Sigma\text{Fe}$.

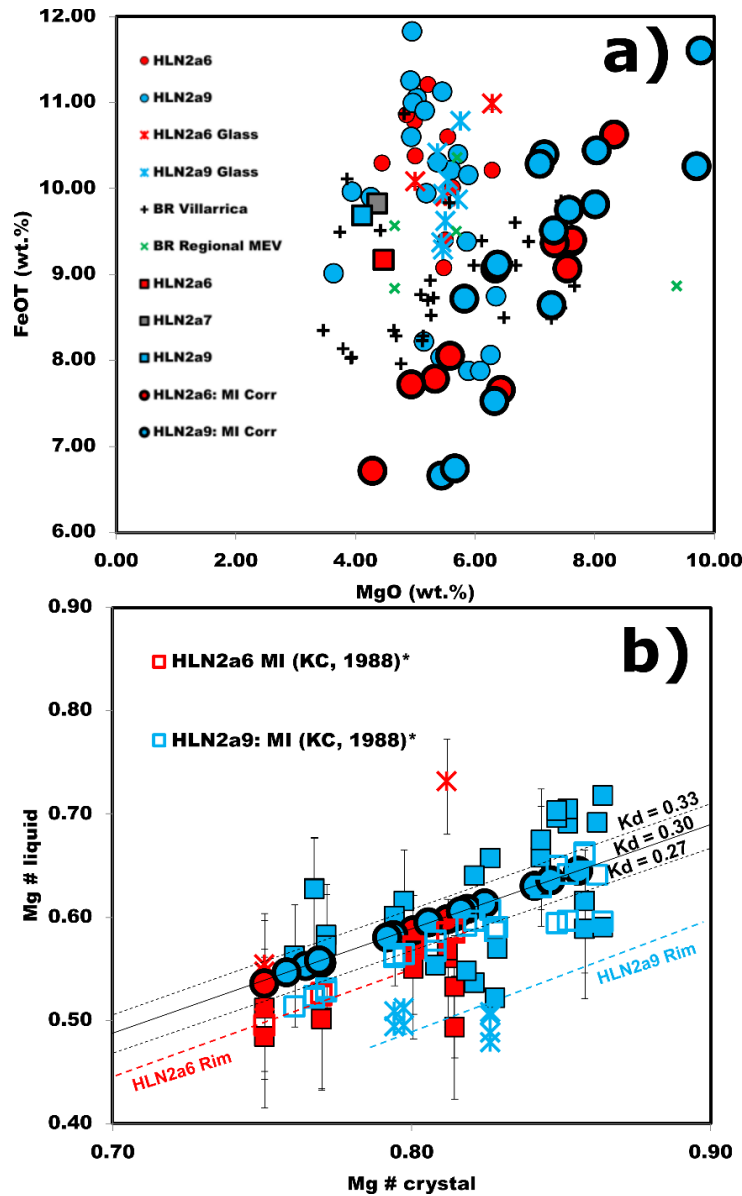


Figure 1. Post entrapment crystallization corrections of olivine-hosted melt inclusions. Literature data from Villarrica are represented by black cross [9-13], while minor eruptive vents (MEV) from the regional sector close to Villarrica are illustrated with a green X symbol [14-17]. a) **FeOT versus MgO diagram** (see also Figure 3 for symbols). Uncorrected PEC MIs that are represented by filled circles, matrix glasses by "X", where bulk rock literature data from Villarrica and MEV found nearby Villarrica are compared. Bulk rock data from this study are represented by filled color squares. b) **Mg# liquid versus Mg# crystal** (or forsterite content Fo% from olivine) where average crystal glass rims compositions are represented for the series HLN2a6 (red dotted line) and HLN2a9 (blue dotted line). The original MIs data has color center representing total iron species with Fe^{2+} neglected. Those filled squares demonstrate error bars for which the minimum and maximum Mg# liquid values represent the minimum or maximum Fe^{2+} content that would be used to calculate Mg# (supposing if both iron species are present). The unfilled squares are PEC-corrected MIs produced by Petrolog 3 without being adjusted for KD (KC*model of Kress and Carmichael, 1988, [3]). The filled circles are PEC corrected MIs adjusted to fit a perfect equilibrium ($KD = 0.30$)[18].

References

- [1] Danyushevsky, L. V. and P. Plechov, (2011). Petrolog3: integrated software for modeling crystallization processes. *Geochemistry, Geophysics, Geosystems*, Vol. 12
- [2] Saikkonen, R. J. and I.A. Rautiainen (1993). Determination of ferrous iron in rock and minerals samples by three volumetric methods, *Bull. Geol. Soc. Finland* 65. Part 1, p. 59–63
- [3] Kress, V. C., & Carmichael, I. S. (1988). Stoichiometry of the iron oxidation reaction in silicate melts. *American Mineralogist*, 73(11-12), p. 1267–1274
- [4] Jugo, P.J., 2009. Sulfur content at sulfide saturation in oxidized magmas. *Geology* 37 (5), 415–418
- [5] Danyushevsky, L.V., F.N. Della-Pasqua, S. Sokolov, (2000). Re-equilibration of melt inclusions trapped by magnesian olivine phenocrysts from subduction-related magmas: petrological implications. *Contrib Mineral Petrol*, Vol. 138, p. 68–83
- [6] Danyushevsky, L.V., A. W. McNeill, A. V. Sobolev, (2002b). Experimental and petrological studies of melt inclusions in phenocrysts from mantle-derived magmas: An overview of techniques, advantages and complications, *Chem. Geol.*, Vol. 183, p. 5–24
- [7] Toplis, M. J. (2005). The thermodynamics of iron and magnesium partitioning between olivine and liquid: Criteria for assessing and predicting equilibrium in natural and experimental systems, *Contrib. Mineral. Petrol.*, Vol. 149, p. 22–39
- [8] Ejima T., Y. Osanai, M. Akasaka, T. Adachi, N. Nakano, Y. Kon, H. Ohfuji, J. Sereenen (2018). Oxidation states of Fe in constituent minerals of a spinel lherzolite xenolith from the Tariat Depression, Mongolia: the significance of Fe³⁺ in olivine. *Minerals* 8:204
- [9] Tormey, D. R., Hickey-Vargas, R., Frey, F. A., & López-Escobar, L. (1991). Recent lavas from the Andean volcanic front (33 to 42 S); interpretations of along-arc compositional variations. *Andean magmatism and its tectonic setting: Geological Society of America Special Paper*, 265, p. 57–77
- [10] Costantini, L., Pioli, L., Bonadonna, C., Clavero, J., & Longchamp, C. (2011). A late Holocene explosive mafic eruption of Villarrica volcano, Southern Andes: the Chaimilla deposit. *Journal of Volcanology and Geothermal Research*, 200(3-4), 143–158
- [11] Wehrmann, H., & Dzierma, Y. (2011). Applicability of statistical eruption analysis to the geological record of Villarrica and Lanín volcanoes, Southern Volcanic Zone, Chile. *Journal of volcanology and geothermal research*, 200(3-4), p. 99–115
- [12] Pioli, L., Scalisi, L., Costantini, L., Di Muro, A., Bonadonna, C., & Clavero, J. (2015). Explosive style, magma degassing and evolution in the Chaimilla eruption, Villarrica volcano, Southern Andes. *Bulletin of Volcanology*, 77(11), p. 1–14
- [13] Held, S., Schill, E., Schneider, J., Nitschke, F., Morata, D., Neumann, T., & Kohl, T. (2018). Geochemical characterization of the geothermal system at Villarrica volcano, Southern Chile; Part 1: Impacts of lithology on the geothermal reservoir. *Geothermics*, 74, p. 226–239
- [14] Gill, J. B. (1981). What is “Typical Calcalkaline Andesite”? In *Orogenic Andesites and Plate Tectonics* (pp. 1-12). Springer, Berlin, Heidelberg.

- [15] Morgado, E., Parada, M. A., Contreras, C., Castruccio, A., Gutiérrez, F., & McGee, L. E. (2015). Contrasting records from mantle to surface of Holocene lavas of two nearby arc volcanic complexes: Caburgua-Huelemolle Small Eruptive Centers and Villarrica Volcano, Southern Chile. *Journal of Volcanology and Geothermal Research*, 306, p. 1–16
- [16] Hickey-Vargas, R., Roa, H. M., Escobar, L. L., & Frey, F. A. (1989). Geochemical variations in Andean basaltic and silicic lavas from the Villarrica-Lanin volcanic chain (39.5 S): an evaluation of source heterogeneity, fractional crystallization and crustal assimilation. *Contributions to Mineralogy and Petrology*, 103(3), p. 361–386
- [17] Hickey-Vargas, R., Sun, M., López-Escobar, L., Moreno-Roa, H., Reagan, M. K., Morris, J. D., & Ryan, J. G. (2002). Multiple subduction components in the mantle wedge: evidence from eruptive centers in the Central Southern volcanic zone, Chile. *Geology*, 30(3), p. 199–202
- [18] Roeder, P.L. and R. Emslie (1970). Olivine-liquid equilibrium, *Contrib Mineral Petrol.* 29, p. 275–289